

1 **Supporting information**

2

3

4 **Influence of North Pacific Decadal Variability on the Western Canadian**  
5 **Arctic over the past 700 years**

6

7 **Text 1**

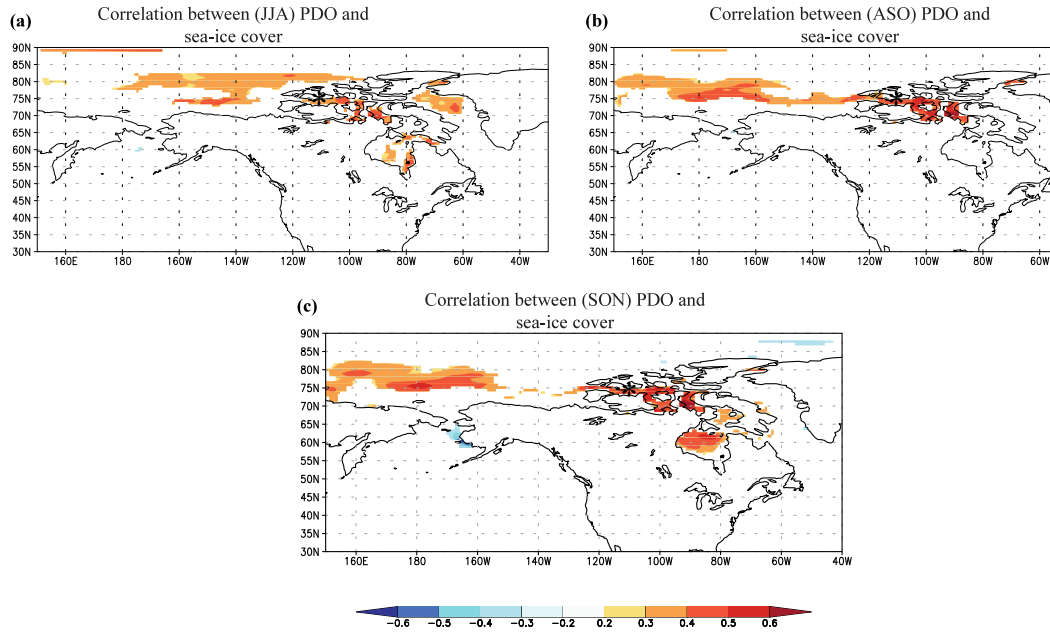
8 **Chronological control**

9

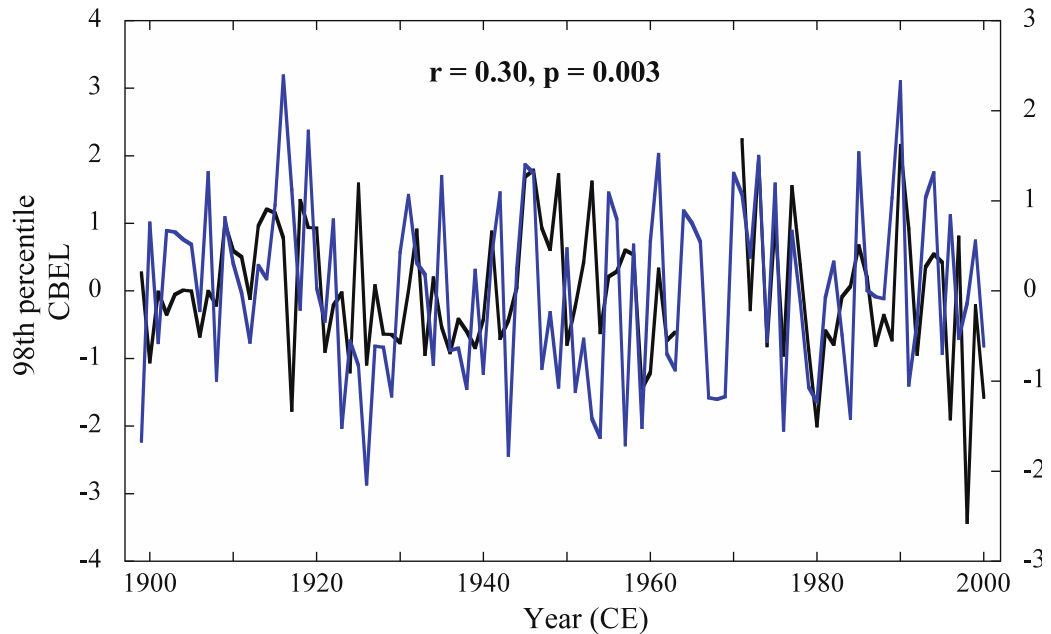
10           The methods used to count varves rely on both visual examination of thin  
11 sections and the use of ~ 7000 microscopic images (1024 X 768  $\mu\text{m}$ ) obtained using a  
12 scanning electron microscope in backscattered mode. This technique allows for the  
13 identification of thin varves ( $< 0.4 \text{ mm}$ ), thus decreasing the chances of missing thin  
14 varves (Ojala et al., 2012). The chronology of the recent part of the record was also  
15 confirmed by radiometric dating ( $^{137}\text{Cs}$  and  $^{210}\text{Pb}$ ) (Cuven et al., 2011). Counts were  
16 made by two different users and yielded very similar results in the upper part (above 167  
17 cm), in which the first 925 varves are present (1075 CE). The error between the two  
18 counts is estimated to be lower than 1.2% (Lapointe et al., 2012), a very good number  
19 compared to other similar records (Ojala et al., 2012). Overall, the counts were very  
20 consistent since 244 CE implying that the varves from Cape Bounty East Lake are well-  
21 defined and unambiguous (Lapointe et al., 2012). Only three coarse layers, dated 1971  
22 (Lapointe et al. 2012), 1446 CE (Fig. S4) and 1300 CE (Fig. S6), are found in the 1766-  
23 year long sequence. These are the sole discernible features that have likely caused minor  
24 erosion in our sedimentary record from 1300-2000 CE (Figs. S4, S6). Moreover, Ct-  
25 Scans of the core did not reveal any hiatus or unconformity. Finally a recent acoustic  
26 survey revealed that the coring site was devoid of mass movement deposits (Normandeau  
27 et al., 2016b). In brief, all these features are suggesting that our sedimentary record is  
28 minimally affected by erosion (Cuven et al., 2011; Lapointe et al., 2012).

29 For wavelet analysis (Fig.5), we use the interval 244-2000 CE as the lake was fully  
30 isolated by glacioisostatic uplift from the ocean after 244 CE (Cuven et al., 2011;  
31 Lapointe et al., 2012). We note a weaker correlation between our record and the PDO-  
32 reconstruction (Macdonald et al., 2005) prior to ~1300 CE during a period that  
33 corresponds broadly with a thick erosive layer dated ~1300 CE in the varve chronology  
34 (Lapointe et al., 2012) (Fig. S6). This layer has been suggested to be the consequence of  
35 a mass movement deposit in a recent study (Normandeau et al., 2016a). However, this  
36 event is also relatively synchronous with an unprecedented negative anomaly in the  
37 reconstructed PDO occurring around 1296 CE (Macdonald et al., 2005). Cross-  
38 correlation between these two proxy records shows a significant correlation between  
39 993-1299 CE when VT is shifted by 45 years (CBEL lags PDO by 45 years,  $r = -0.20$ ,  $p$   
40  $< 0.001$ ; Fig. S7), suggesting that the large debris flow at ~1300 CE likely eroded 45  
41 varves. It is worth noting that the tree-ring based PDO reconstruction values prior to  
42 1300 CE are almost constantly negative. Moreover, the period encompassing 1000-1300  
43 CE is characterized by periods of massive droughts in the southwestern USA, causing a  
44 deficit of soil-water recharge and possibly widespread tree mortality in this region  
45 (Williams et al., 2013). In any case, the low distribution of tree-rings prior to 1300 CE  
46 impedes a good understanding of the climate in the Northern latitudes (Wilson et al.,  
47 2015).

48

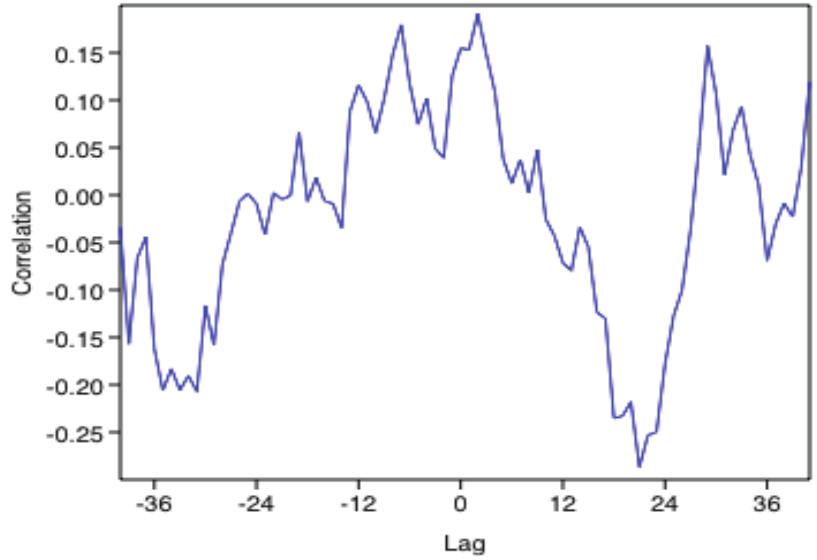


49  
 50 **Figure S1.** Sea-ice cover anomalies in relation to PDO phases during summer  
 51 and autumn. Correlation between PDO (Huang et al., 2015) and sea-ice anomalies  
 52 from ERA-Interim (Dee et al., 2011) for June-August (a), August-October (b),  
 53 and September-November (c) during 1979-2016. Black asterisk denotes Cape  
 54 Bounty.  
 55



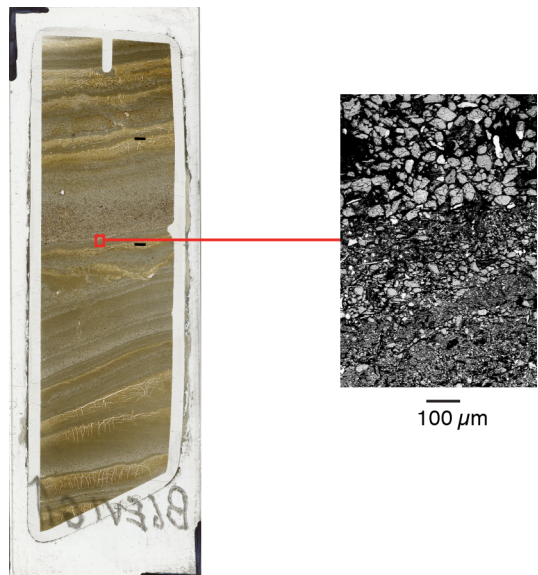
56  
 57 **Figure S2.** Correlation between the 98<sup>th</sup> percentile at CBEL (Lapointe et al.  
 58 2012) and the NPI during September-November (Trenberth and Hurrell 1994) for  
 59 the past 100 years.

### PC1 of PDOs versus CBEL VT



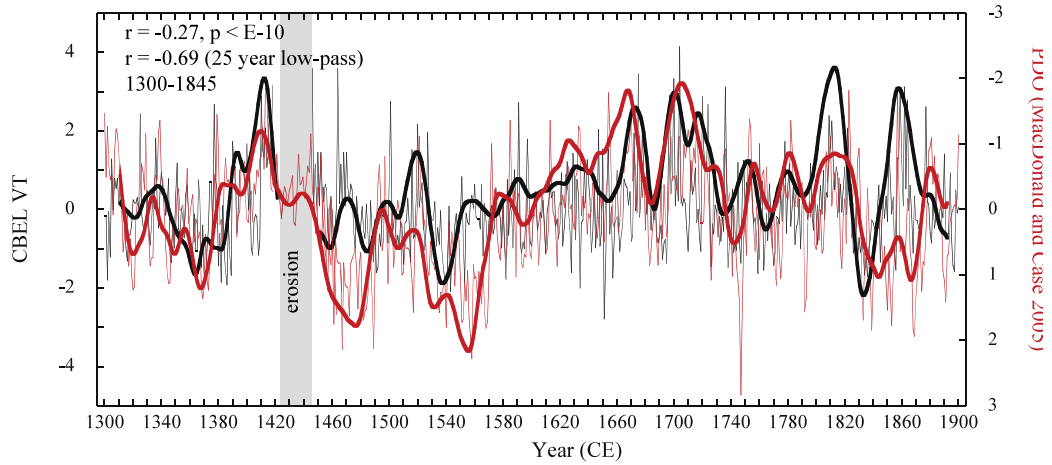
60  
61  
62  
63  
64  
65  
66  
67

**Figure S3.** Cross-correlation between annual PC1 of reconstructed PDOs (MacDonald and Case 2005), D’Arrigo et al. 2001, Gedalof and Smith 2001) versus annual CBEL varve thickness from 1700-1900. Maximum correlation is reached at 18 year lag, that is CBEL leads the PDO reconstructions.



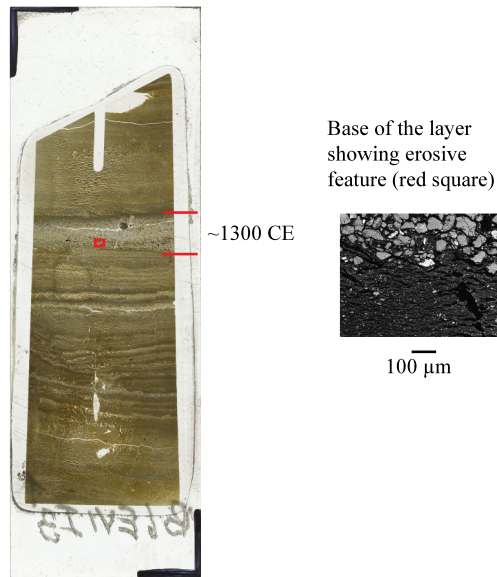
68  
69  
70  
71  
72  
73

**Figure S4.** Large turbidite showing erosive features. The black lines indicate the thickness of the layer (1.34 cm) dated to 1446 CE. The backscattered electron image acquired at the scanning electron microscope shows the base of the turbidite (red square). Core # CBEV1, depth from top: 101.88 cm.



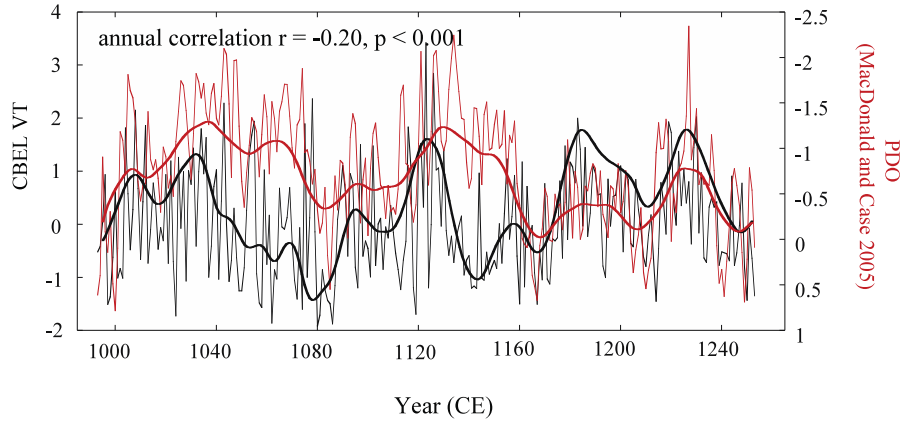
74  
75  
76  
77  
78  
79  
80  
81

**Figure S5.** Comparison between CBEL varve thickness and the Pacific Decadal Oscillation (Macdonald et al., 2005) over the last ~700 years. Bold lines are 25-year low-pass filter. Grey shading (b) indicates the 28 years eroded varves at CBEL.

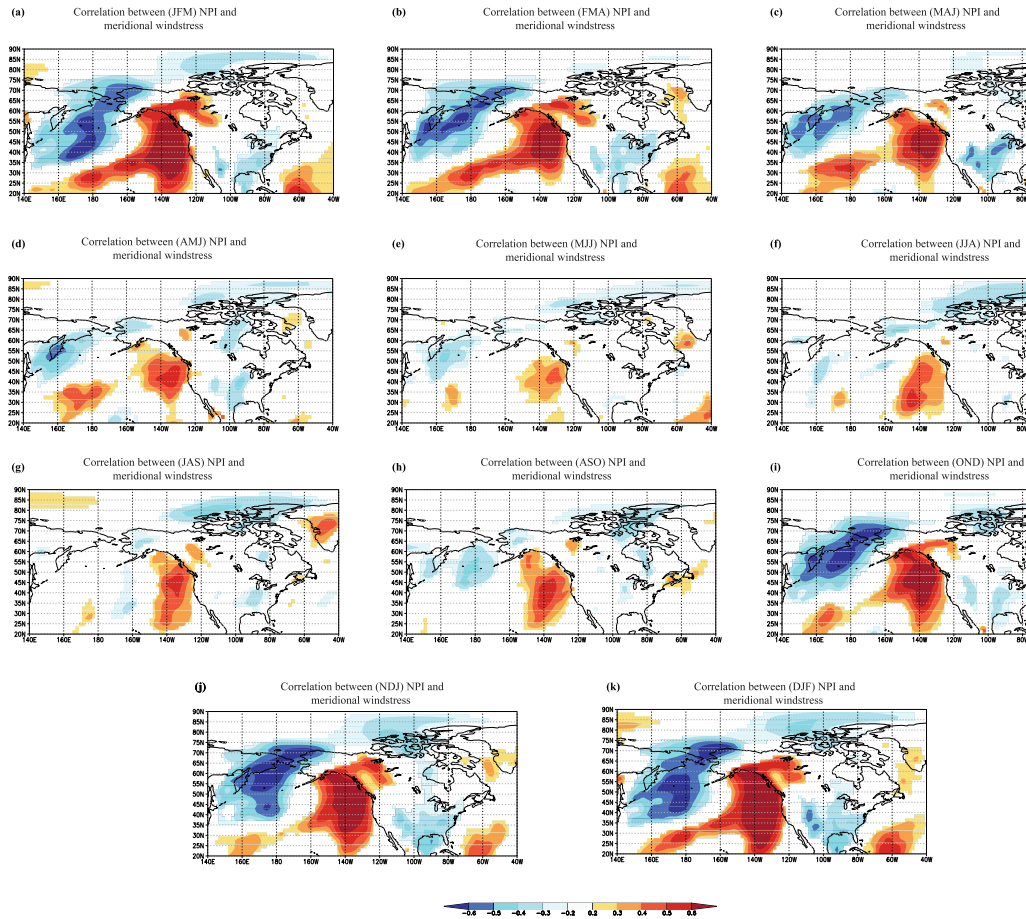


82  
83  
84  
85  
86  
87  
88  
89  
90

**Figure S6.** Largest debris flow deposit dated to ~1300 CE. The backscattered electron image acquired at the scanning electron microscope shows the base of the debris flow (red square). Core # CBEV1, depth from top: 130.14 cm.



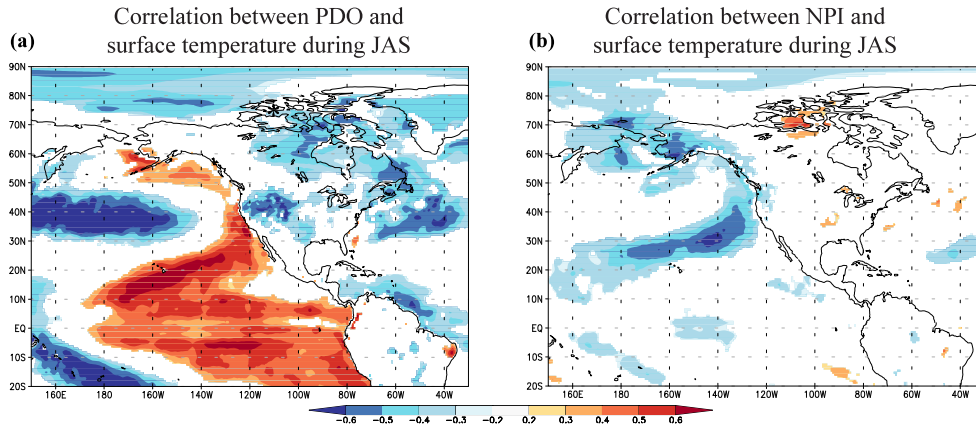
91  
 92 **Figure S7.** Varve thickness versus reconstructed PDO(Macdonald et al., 2005)  
 93 during the Medieval Climate Anomaly. Bold lines are 25-year low-pass filter.  
 94 Varve thickness is shifted 45 years earlier.  
 95  
 96  
 97  
 98  
 99  
 100  
 101



102  
 103  
 104  
 105  
 106  
 107  
 108  
 109  
 110  
 111

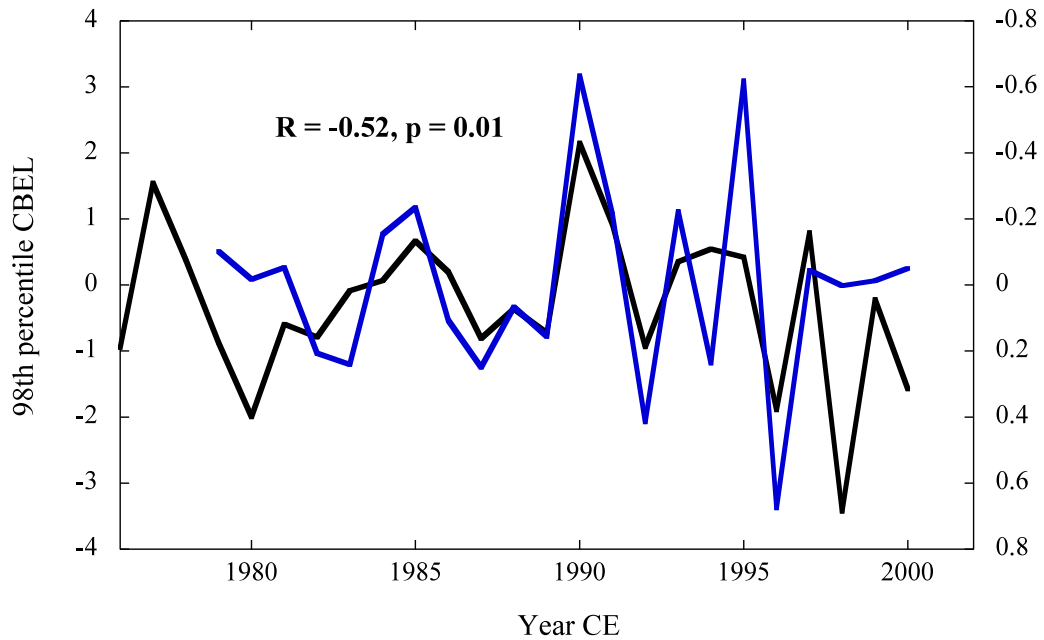
**Figure S8.** Same as Figure 6a, but for all year-round except SON (as it is in the main text). (a) averaged January-March, (b) February-April, (c) March-May, (d) April-June, (e) May-July, (f) June-August, (g) July-September, (h) August-October, (i) October-December, (j) November-January and (k) December-February.

112  
 113  
 114  
 115  
 116  
 117  
 118



119  
120  
121  
122  
123  
124  
125  
126

**Figure S9.** North Pacific influences on temperature anomalies in the western Canadian Arctic. (a), Spatial correlation between July-September PDO index and July-September surface temperature (Dee et al., 2011) for 1979-2016. (b), as in (a), but for the North Pacific Index (Trenberth et al., 1994).



127  
128  
129  
130  
131  
132  
133  
134  
135  
136  
137

**Figure S10.** Summer sea ice extent covering 84°- 67°N / 100° W - 170° E compared to the 98<sup>th</sup> percentile at CBEL.



- 138 **References**  
139  
140 Cuven, S., Francus, P. and Lamoureux SF.: Mid to Late Holocene hydroclimatic and  
141 geochemical records from the varved sediments of East Lake, Cape Bounty,  
142 Canadian High Arctic, *Quatern. Sci. Rev.*, 30 2651-2665, 2011.
- 143 Dee, D., S. Uppala, A., Simmons, P., Berrisford, P., Poli, S., Kobayashi, U., Andrae, M.,  
144 Balmaseda, G., Balsamo and Bauer P.: The ERA-Interim reanalysis:  
145 Configuration and performance of the data assimilation system, *Q. J. R.*  
146 *Meteorol. Soc.*, 137, 553-597, 10.1002/qj.828, 2011.
- 147 Huang, B., Banzon, V. F., Freeman, E., Lawrimore, J., Liu, W., Peterson, T.C., Smith,  
148 T.M., Thorne, P.W., Woodruff, S.D. and Zhang, H.-M.: Extended reconstructed  
149 sea surface temperature version 4 (ERSST. v4), Part I: upgrades and  
150 intercomparisons, *J. Climate*, 28, 911-930, 2015.
- 151 Lapointe, F., Francus, P., Lamoureux, SF., Saïd, M. and Cuven, S.: 1750 years of large  
152 rainfall events inferred from particle size at East Lake, Cape Bounty, Melville  
153 Island, Canada, *J. Paleolimnol.*, 48, 159-173, doi: 10.1007/s10933-012-9611-8,  
154 2012.
- 155 MacDonald, G. M. and Case, R.A.: Variations in the Pacific Decadal Oscillation over the  
156 past millennium, *Geophys. Res. Lett.*, 32, 10.1029/2005GL022478, 2005.
- 157 Normandeau A., Joyal G., Lajeunesse P., Francus P., Lamoureux SF. and Lapointe F.:  
158 Late-Holocene Mass Movements in High Arctic East Lake, Melville Island  
159 (Western Canadian Arctic Archipelago). *Submarine Mass Movements and their*  
160 *Consequences*: Springer; 2016. p. 311-20.  
161
- 162 Normandeau, A., Lamoureux, SF., Lajeunesse, P. and P. Francus.: Sediment dynamics  
163 in paired High Arctic lakes revealed from high-resolution swath bathymetry and  
164 acoustic stratigraphy surveys, *J. Geophys. Res.: Earth Surface.*, 2016b.  
165
- 166 Ojala, A., Francus, P., Zolitschka, B., Besonen M., and Lamoureux, SF.: Characteristics  
167 of sedimentary varve chronologies—a review, *Quatern. Sci. Rev.*, 43, 45-60, 2012.
- 168 Trenberth, K. E. and Hurrell, J.W.: Decadal atmosphere-ocean variations in the Pacific.  
169 *Clim. Dynam.*, 9, 303-319, doi:10.1007/BF00204745, 1994.
- 170 Williams, A. P., Allen, C.D., Macalady, AK., Griffin, D., Woodhouse, C.A., Meko, D.M.,  
171 Swetnam, T.W., Rauscher, S.A., Seager, R. and Grissino-Mayer, H.D.:  
172 Temperature as a potent driver of regional forest drought stress and tree mortality,  
173 *Nature Clim. Change*, 3(3), 292-297, 2013.  
174
- 175 Wilson, R., K. Anchukaitis, K. Briffa, U. Büntgen, E. Cook, R. D'Arrigo, J. Esper, D.  
176 Frank, B. Gunnarson, and G. Hegerl (2015), Are tree-ring based estimates for  
177 Northern Hemisphere medieval temperatures fit for purpose?, paper presented at  
178 EGU General Assembly Conference Abstracts.  
179